Pamukkale Univ Muh Bilim Derg, 31(8), 1374-1382, 2025
(Special Issue of the 10th Geochemistry Symposium)

Pamukkale Üniversitesi Mühendislik Bilimleri Dergisi

Pamukkale University Journal of Engineering Sciences

Hydrogeochemistry and origin of carbonated, sulfated, and saline geothermal waters, Central Anatolia, Türkiye

Orta Anadolu'daki karbonatlı, sülfatlı ve tuzlu jeotermal suların hidrojeokimyası ve kökeni, Türkiye

Mustafa Afşin[1*], *Mustafa Murat Kavurmacı*[1], *Ali Gürel*[2], *Ümmühan Gökçen Duru*[3], *Özcan Oruç*[4]

[1]Department of Geological Engineering, Faculty of Engineering, Aksaray University, Aksaray, Türkiye.
mafsinbaglum@gmail.com, muratkavurmaci@aksaray.edu.tr
[2]Department of Geological Engineering, Faculty of Engineering, Niğde Ömerhalis Demir University, Niğde, Türkiye.
agurel_1999@yahoo.com
[3]Republic of Türkiye Ministry of Environment, Urbanization and Climate Change, Ankara, Türkiye.
gokcenduru@hotmail.com
[4]Department of Environmental Engineering, Faculty of Engineering, Aksaray University, Aksaray, Türkiye.
ozcanoruc68@gmail.com

Received/Geliş Tarihi: 27.09.2025 Revision/Düzeltme Tarihi: 10.11.2025 doi: 10.65206/pajes.84780
Accepted/Kabul Tarihi: 10.11.2025 Special Issue Article/Özel Sayı Makalesi

Abstract

This study aims to compare the geothermal waters of Gümüşkent (GK), Koçpınar (KP), Dertalan (DA), Terme (TE), Kozaklı (KZ), Bayramhacı (BH), Karakaya (KK), Tuzlusu (TZ), Ziga (ZG), Narlıgöl (NG), Yeşilhisar (YH), and Kemerhisar (KH), which exhibit temperatures ranging from 17.5 °C to 86 °C. Additionally, the origins of these waters are evaluated by taking into account the cold waters of Helvadere (HD), Dokuzpınar (DP), Terme (TES), and Kozaklı (KOS), with temperatures between 10.4 °C and 13.09 °C, all located in Central Anatolia. The aquifers of these fault-controlled waters are of Paleozoic marbles and Eocene limestones; cover rocks are impermeable units. The heat production system of these waters may be due to young volcanism and granitic/syenitic intrusions as well as radiogenic sources. The types of these carbonated, sulfated, and saline waters are Ca-HCO_3 in KP, GK, BH, and TE; Na-SO_4 in KZ; Ca-SO_4 in DA; Na-Cl in TZ, ZG, NG, KH, KK, and YH, respectively. These waters, which are of meteoric origin in terms of isotopic ($\delta^{18}O$ and $\delta^{2}H$), generally have deep circulation and slow flow. The main reason for the deviation observed from the meteoric water line in some waters is evaporation. In KH, YH, and KK with low temperatures, the mineralization of these waters increased as a result of long-term gas-rock-water interaction. The causes of salinization in the Na-Cl-type waters may be the dissolution of halite minerals and the mixing of older waters trapped at depth during the closure of the Tuzgölü and salt domes in the TZ and ZG, the Central Kızılırmak basin in the YH and KK, and the Ulukışla basin in the KH. According to $\delta^{13}C$ (‰PDB) values, the sources of CO_2 gas in waters may be geogenic (marble, marine and lacustrine limestone) and/or mantle. According to $\delta^{34}S$‰VCDT values, the source of sulfate in waters may be evaporitic rocks in KK, ZG, KZ, TZ, KH, and volcanic and/or carbonate rocks in other waters. The 14C ages of the waters are lowest in DA (19.15 ka) and highest in KK (45.11 ka). The calculated ages are apparent because the ^{14}C values of the waters in question are often a measure of the contribution of modern biogenic carbon to the total dissolved carbonate or bicarbonate. In this context, the waters examined may be old waters that entered the system from the late Pleistocene to the early Holocene periods.

Keywords: Geothermal waters, Carbon and sulfur isotopes, Hydrogeochemistry, Central Anatolia.

Öz

Bu çalışmanın amacı, Orta Anadolu'da sıcaklıkları 17.5 – 86 °C arasında değişen Gümüşkent (GK), Koçpınar (KP), Dertalan (DA), Terme (TE), Kozaklı (KZ), Bayramhacı (BH), Karakaya (KK), Tuzlusu (TZ), Ziga (ZG), Narlıgöl (NG), Yeşilhisar (YH) ve Kemerhisar (KH) jeotermal sularını, bu jeotermal suların bulunduğu alanlarda, sıcaklıkları 10.4 ile 13.09 °C arasında değişen Helvadere (HD), Dokuzpınar (DP), Terme (TES) ve Kozaklı (KOS) soğuk suları da dikkate alarak su kimyası ve su izotopları yardımıyla karşılaştırmak ve kökenlerini değerlendirmektir. Fay kontrollü bu suların akiferleri Paleozoyik yaşlı mermerler ve Eosen yaşlı kireçtaşları; örtü kayaları ise geçirimsiz birimlerdir. Bu suların ısı üretim sistemi genç volkanizma ve granitik/siyenitik sokulumların yanı sıra radyojenik kaynaklara da bağlı olabilir. Karbonatlı, sülfatlı ve tuzlu bu suların tipleri KP, GK, BH ve TE'de Ca-HCO_3; KZ'de Na-SO_4; DA'da Ca-SO_4; TZ, ZG, NG, KH, KK ve YH'da Na-Cl şeklindedir. İzotopik ($\delta^{18}O$ ve $\delta^{2}H$) açıdan meteorik kökenli olan bu sular genelde derin dolaşımlı ve yavaş akışlıdır. Bazı sularda meteorik su doğrusundan gözlenen sapmanın asıl nedeni buharlaşmadır. Sıcaklığı düşük KH, YH ve KK'nın mineralizasyonları uzun süreli gaz-kayaç-su etkileşimi sonucu yükselmiştir. Na-Cl tipli sularda tuzlanmanın sebepleri halit mineralinin çözünmesi ile TZ ve ZG'de Tuzgölü ve tuz domları, YH ve KK'da Orta Kızılırmak ve KH'da Ulukışla havzalarının kapanımı sırasında derinlerde kalmış daha yaşlı suların bu sulara karışması olabilir. $\delta^{13}C$ (‰PDB) değerlerine göre sulardaki CO_2 gazının kaynağı, jeojenik (mermer, denizel ve gölsel kireçtaşı) ve/veya manto olabilir. $\delta^{34}S$ ‰VCDT değerlerine göre sulardaki sülfatın kaynağı KK, ZG, KZ, TZ, KH'da evaporitik, diğer sularda ise volkanik ve/veya karbonat kayaçlar olabilir. Suların ^{14}C yaşları DA'da en düşük (19.15 ka), KK'da en yüksektir (45.11 ka). Söz konusu suların ^{14}C değerleri çoğunlukla toplam çözünmüş karbonat veya bikarbonattaki modern biyojenik karbonun katkısının ölçümü olduğu için hesaplanan yaşlar görünürdür. Bu bağlamda, incelenen sular geç Pleyistosen ve erken Holosen döneminde sisteme girmiş yaşlı sular olabilir.

Anahtar kelimeler: Jeotermal sular, Karbon ve sülfür izotopları, Hidrojeokimya, Orta Anadolu.

*Corresponding author/Yazışılan Yazar

1 Introduction

Türkiye lies within the active Alpine-Himalayan orogenic belt, with numerous tectonic features, including grabens, active fault lines, hydrothermal alteration zones, and geothermal areas. The distribution of thermal waters in Türkiye is largely controlled by active fault structures and their association with hydrothermally altered terrains of Tertiary–Quaternary magmatic origin [1]-[3]. Central Anatolia is rich in geothermal energy resources.

In this study, some important geothermal waters such as Gümüşkent (GK), Koçpınar (KP), Dertalan (DA), Terme (TE), Kozaklı (KZ), Bayramhacı (BH), Karakaya (KK), Tuzlusu (TZ), Ziga (ZG), Narlıgöl (NG), Yeşilhisar (YH), and the cold waters such as Helvadere (HD), Dokuzpınar (DP), Terme (TES), and Kozaklı (KOS) in central Anatolia are selected (Figure 1).

Geothermal water temperatures (°C) change from 17.5 to 86, whereas cold waters exhibit a narrower temperature (°C) interval of 10.4–13.09. In this context, [4] classified the KP spring waters as *mineral waters* owing to their high free CO_2 content (870–2145 mg/L). The temperatures of these waters have been reported as 20 °C [5] and 25 °C [6] in previous studies. Deep drilling operations-some exceeding 3000 m in depth–conducted by a private company in and around the KP spring area between 2022 and 2025 also revealed temperatures above 20 °C. The KP spring waters are further characterized by elevated CO_2 concentrations and recognized therapeutic properties [7]. Accordingly, in the present study, the KP area was evaluated within the framework of geothermal waters. These waters are evaluated from hydrogeochemistry and water isotopes ($\delta^{18}O$, $\delta^{2}H$, $\delta^{13}C$, $\delta^{34}S$, ^{3}H, and $\delta^{14}C$) perspectives (Figure 1).

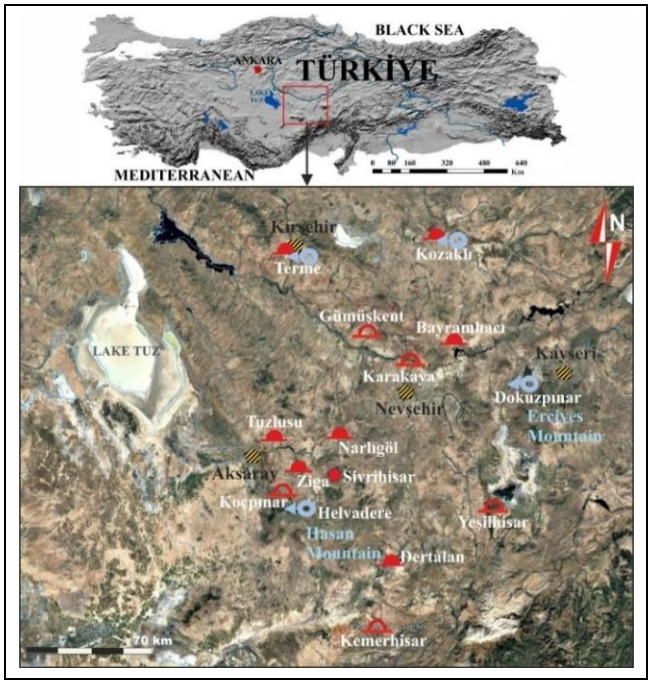

Figure 1. Location map of the study area.

The geology, hydrogeology, and isotopic characteristics of the areas where geothermal waters are found were largely utilized in this study by [8] and [2].

The objective of this study is to compare geothermal waters and evaluate their origins by incorporating cold waters into the analysis, estimating recharge elevations and temperatures, determining the origins of carbon and sulfur in groundwater, and constraining groundwater residence times using radiocarbon and tritium data.

2 Geology and Hydrogeology

The basements of the study areas are formed by Bozçaldağ metamorphics consisting of Pre-Mesozoic marble, gneisses, and quartzites, and are overlain by units with lithologies ranging in age from Cenozoic to Quaternary (Figure 2). These units have different hydrogeological features. Of the basement units in question, massive marble and schists are impermeable, while marbles containing discontinuities and where karstification has generally developed are permeable. All cold, geothermal (mineralized, thermal, and mineralized) waters examined emerge in relation to discontinuities in their recharge areas, and the origin of geothermal waters is most likely the marbles in the confined aquifer position. Except for the weathered and fractured levels of granitoids and ophiolites outcropping in some areas, which are permeable, tuffs, ashes, and clays are completely impermeable and act as cap rocks. Carbonate-cemented or loosely consolidated conglomerate, sandstone, and limestone levels of the terrestrial and lacustrine units are permeable; claystone levels are impermeable; silty levels are semi-permeable. Volcanic rocks are generally impermeable; basalts and ignimbrites are permeable in the vertical direction, depending on the depth of open fractures. Gravel, sand, sandstone, and carbonate - cemented conglomerates carried by streams are permeable; clay-bearing levels are impermeable; slope debris and old and new alluvium are permeable except for clayey levels. The aquifers of these fault-controlled waters are of Paleozoic marbles and Eocene limestones; cover rocks are impermeable units. The heat production system of these waters may be due to young volcanism and granitic/syenitic intrusions as well as radiogenic sources [8].

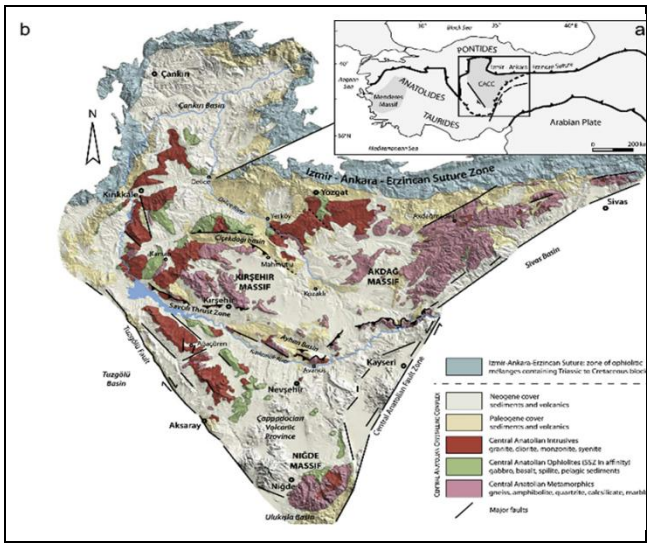

Figure 2. (a): Location of the Central Anatolian Crystalline Complex (CACC) in the Turkish orogenic system.
(b): Simplified geological map of the CACC projected on a Digital Elevation Model (not to scale) (After [9]).

3 Materials and methods

pH and specific electrical conductivity measurements (SEC, µS/cm at 25 °C) were performed on-site using a multi-parameter probe, which was calibrated before the campaign during field measurements. Water temperature (T) (°C) was determined with a factory-calibrated thermocouple. In total, 31 samples were obtained from 16 different locations for subsequent chemical and isotopic analyses.

Sampling was conducted during the wet season (May 2005, 1 numbered samples) and the dry season (November 2005, 2 numbered samples). Water samples for cation analysis were collected in 500 mL polyethylene (PE) bottles with double caps and acidified to pH ≤ 2 using 0.1 M HNO_3. Samples intended for anion analysis were stored under refrigerated conditions until laboratory processing. For isotope analyses ($\delta^{18}O$, $\delta^{2}H$, ^{3}H, $\delta^{13}C$, ^{14}C, and $\delta^{34}S$), samples were also collected in 500 mL double-capped PE bottles, while 1000 mL PE bottles were used specifically for ^{14}C analysis. All sampling followed standard procedures described in [10].

Hydrochemical analyses were carried out at the water chemistry laboratory of Hacettepe University (HU) in Ankara according to the [11] standard methods. Ca^{2+}, Mg^{2+}, Na^{+}, K^{+}, Cl^{-}, and SO_4^{2-} ions by ion chromatography, and for HCO_3^{-} and CO_3^{-} were analyzed by titrimetry techniques. The stable water isotopes ($\delta^{18}O$ and $\delta^{2}H$) were analyzed at the Isotope Laboratory in the Ankara Technical Research-Quality Control (TAKK) Directorate of the State Hydraulic Works (DSI) by using Isotope Ratio Mass Spectrometry.

Tritium (^{3}H) measurements of the groundwaters were fulfilled at the HU Environmental Tritium Laboratory using an ultra-low-level liquid scintillation technique, while radiocarbon (^{14}C) measurements were done exclusively in the dissolved inorganic carbon fraction, with analyses performed via accelerator mass spectrometry at Geochron Laboratories, University of Massachusetts, USA. Carbon isotopes ($\delta^{13}C$) were also determined by accelerator mass spectrometry on a portion of the same sample. Sulfur isotope ratios ($\delta^{34}S$) were analyzed at the Nevada Stable Isotope Laboratory (USA) and reported relative to Canyon Diablo Troilite (CDT), while $\delta^{13}C$, $\delta^{18}O$, and $\delta^{2}H$ values were referenced to the Vienna Pee Dee Belemnite (VPDB) and Vienna Standard Mean Ocean Water (VSMOW), respectively.

4 Results and discussion

4.1 Hydrogeochemistry

The pH ranges from 5.57 to 7.25 in cold waters and 4.92 to 7.25 in geothermal waters in the study area. T (°C) gives an order of 10.4–13.9 in cold waters and 17.5–86 in geothermal waters. SEC (µS/cm) changes between 207 and 681 in cold waters and between 586 and 17400 in geothermal waters. DO (mg/L) shifts between 3.2–17.55 in cold waters and 0.13–13.4 in geothermal waters (Table 1).

Groundwater is typically classified based on its residence time within geological formations-recently recharged water is termed 'young,' while water that has remained underground for longer periods is considered 'old.' Generally, groundwater temperature and dissolved-solids concentration increase with depth and with longer residence times [10]. But, this pattern can reverse in some cases, particularly when shallow geological layers contain more soluble minerals than deeper ones, resulting in higher dissolved solids concentrations in shallow groundwater [3] (Figure 3a). Four hydrochemical facies are classified [12] using cation and anion concentrations of cold and geothermal waters in this study. These are (1) Ca-HCO_3, (2) Ca-SO_4/Na-SO_4 (3) Na-Cl-HCO_3/Na-HCO_3-Cl (4) Na-Cl (Table 1). Facies 1 (Ca-HCO_3) represent the cold (HD, TES, and KOS) and geothermal groundwaters (KP, BH, and TE). HD circulated in the shallow zones of an unconfined aquifer consists of basalt, with shallow circulation depths have low temperatures (°C) (10.4-13.9) low and SEC (µS/cm) (207-681), KP, BH and TE geothermal waters with deep circulation of confined aquifers consist of marbles have low/high temperatures (18.5-54.3), and high SEC (586 – 2070) values, respectively. During KP's ascent from depth to the surface, mixing with cold waters likely caused a decline in both water temperature and SEC. Facies 2 (Na-HCO_3-Cl/Na-Cl-HCO_3) denotes the DP1 and DP2, respectively. DP has low-SEC (530 to 520 µS/cm) and low temperature (12.5 °C). DP circulated in the shallow zones of an unconfined aquifer consists of basalt. DP indicates a seasonal switch from HCO_3^{-}-dominated water in the rainy season to Cl^{-}-dominated water in the dry season. Because SEC remains nearly constant, the dry-season Cl^{-} increase likely results from mixing with older waters or from anthropogenic contamination (Table 1).

Facies 3 Ca-SO_4/$NaSO_4$ represents DA and KZ geothermal waters. DA has low temperature (28.5-28.6 °C) and low SEC (µS/cm) (705-730) values. Whereas, KZ has high temperature (81-86) and high SEC (2070-3100) values. DA has circulated to a limited extent within intermediate zones of fractured andesites in the Keçiboyduran mountain. In this context, the rotten egg odour in the spring area and alunite deposits observed along the Kükürdün creek in DA indicate the presence of H_2S gas, and the origin of the SO_4^{2-} ion in this water may be the sulfur in the Melendizdağ tuff. The origin of SO_4^{2-} is evaporitic (gypsum) in TZ, ZG, KZ, YH, KH, and KK; it is volcanic in KP and NG; and it is the dissolution of carbonates in TE and BH. In samples like KP, TE, and BH, Ca^{2+} and HCO_3^{-} ions dominate, reflecting the high CO_2 concentration of the waters and the presence of carbonate rock formations in the area. The significant concentrations of Mg^{2+} found in waters like YH indicate interactions with serpentinized ultramafic rocks, gabbros, or basalts (Figure 3a).

Facies 4 Na-Cl represents ZG, YH, TZ, and KK geothermal waters (Table 1 and Figure 3b). A strong positive linear correlation between Na^{+} and Cl^{-} concentrations was identified (r^2 = 0.96). The geothermal waters, which have Na-Cl water types such as KK, KH, YH, TZ, and ZG, are thought to have interacted with evaporitic units, salt domes, and other salt-bearing rocks as they ascended to the surface through the carbonate aquifer.

The elevated salinity in these waters is possibly due to mixing with older, deep groundwater that remained trapped beneath the surface after the closure of basins like Tuzgölü (for TZ and ZG), Kızılırmak (for KK), and Ulukışla (for KH), as well as with mineral-rich waters [13],[8],[2]. In contrast, the lower specific electrical conductivity (SEC) and temperature values observed in other geothermal waters may be attributed to dilution processes caused by mixing with cold groundwater, likely as a result of hyperfiltration [14]. The Na^{+} and Cl^{-} signatures of cold end-member 1 contribute negligibly to the overall mixing dynamics. Additionally, the slow and long circulation processes along the groundwater flow direction have contributed to this enrichment (Figure 3a).

Table 1. Hydrochemical analyses results, ion ratios, and types of the waters (ion values are in meq/L).

Sample Symbol	T	pH	SEC	DO	Ca^{2+}	Mg^{2+}	Na^{+}	K^{+}	Cl^{-}	SO_4^{2-}	HCO_3^{-}	Na/Cl	Water Type
HD1	10.4	7.17	207	10.5	2.51	0.808	0.726	0.054	0.343	0.240	1.55	2.12	Ca-HCO_3
HD2	10.4	5.97	214	12.12	2.76	0.647	0.803	0.053	0.332	0.235	1.62	2.42	
DP1	12.5	6.82	530	8.58	1.14	1.25	2.66	0.133	2.03	0.218	2.41	1.31	Na-HCO_3-Cl
DP2	12.5	6.48	520	17.55	0.995	1.35	2.86	0.144	2.75	0.275	2.2	1.04	Na-Cl-HCO_3
TES1	13.9	7.2	216	3.2	4.86	1.7	0.909	0.053	0.686	1.33	4.96	1.33	
TES2	13.3	7.06	681	7.9	4.75	1.67	0.86	0.048	0.634	1.20	4.59	1.36	
KOS1	20	7.23	300	4.75	9.78	3.47	3.83	0.12	5.36	3.78	6.53	0.71	
KOS2	12.8	7.25	431	13	3.19	0.845	0.307	0.033	0.112	0.162	2.67	2.74	Ca-HCO_3
KP1	20.3	5.76	748	1.98	3.96	1.99	1.46	0.142	0.227	0.173	6.62	6.43	
KP2	18.5	5.57	586	5.4	3.15	1.72	0.78	0.137	0.284	0.25	5.45	2.75	
GK2	17.5	6.5	3160	8.35	30.86	6.41	1.27	0.135	0.088	0.117	37.89	14.43	
NG1	61.1	6.44	5500	2.25	14.31	3.8	11.79	1.36	10.1	2.35	17.47	1.17	Na-Cl
NG2	40	6.29	3200	1.87	14.35	3.9	9.94	1.86	9.62	2.40	17.03	1.03	
DA1	28.5	4.92	705	0.13	4.62	1.21	1.38	0.223	0.344	5.39	1.7	4.03	Ca-SO_4
DA2	28.6	5.25	730	0.84	4.89	1.31	1.46	0.24	0.388	6.07	2.0	3.76	
BH1	43.4	6.15	1903	2.44	13.16	3.11	5.39	0.256	3.82	1.74	14.06	1.41	
BH2	42.2	6.56	1915		13.95	3.39	5.79	0.247	5.17	2.19	13.97	1.12	Ca-HCO_3
TE1	50.2	5.87	1975	0.8	11.66	2.89	6.42	0.257	5.24	1.78	12.05	1.23	
TE2	54.3	6.1	2070	1.23	10.95	3.16	7.46	0.311	5.69	1.87	12.72	1.31	
KZ1	86	6.61	3100	10.13	10.43	2	19.02	0.52	16.38	9.41	4.72	1.16	Na-SO_4
KZ2	81.7	6.22	3010	4.71	8.55	1.75	20.51	0.556	15.35	8.87	5.98	1.34	
ZG1	45.4	5.8	5500	1.14	22.95	3.97	39.88	3.26	38.64	1.13	23.09	1.03	
ZG2	44.7	6.43	6910	2	24.61	1.14	37.29	3.26	36.88	1.37	29.85	1.01	
YH1	15	6.47	9200	2.75	18.77	38.71	56.79	0.824	50.98	16.21	36.58	1.11	
YH2	14.4	6.58	9510	2.7	19.18	40.31	58.46	0.921	66.19	21.62	39.23	0.88	
TZ1	25.9	6.11	5230	1.18	21.83	4.23	30.9	0.823	28.16	1.31	24.79	1.10	Na-Cl
TZ2	25.4	6.15	5710	13.4	21.78	4.32	32.45	0.857	28.37	1.31	25.16	1.14	
KK1	16.9	6.62	16100	3.73	19.54	4.62	160.02	6.4	106.2	5.77	60.89	1.51	
KK2	14.4	6.46	17400	3.2	23.47	5.02	177.87	7.19	115.5	6.88	74.64	1.54	
KH1	14.8	6.12	4200	3.14	12.17	13.67	61.1	0.976	46.56	6.72	24.97	1.31	
KH2	15.6	6.26	7500	2.7	12.67	14.62	69.07	1.09	60.73	9.87	26.60	1.14	

Explanations: T: Temperature (°C), SEC: Specific electrical conductivity, µS/cm, (DO): Dissolved oxygene (mg/L), Cold waters: HD: Helvadere Sp.; DP: Dokuzpınar Sp, TES: Terme cold water drilling, KOS: Kozaklı cold water drilling, KP: Koçpınar Sp.; TZ: Tuzlusu thermal-mineral Sp.; NG: Narlıgöl thermal-mineral drilling; ZSMS: Ziga thermal-mineral drilling; KH: Kemerhisar mineral drilling; DA: Dertalan thermal drilling, YH: Yeşilhisar mineral Sp; BH: Bayramhacı thermal-mineral Sp. KK: Karakaya mineral Sp.; GK2: Gümüşkent mineral Sp.; KZ: Kozaklı thermal-mineral drilling; TE: Terme thermal-mineral drilling; Sampling dates: KK1: 18-21 May 2005 (Rainy season), KK2: 18-21 November 2005 (Dry season). Examples numbered 1 indicate the wet season and numbered 2 indicate the dry season [8].

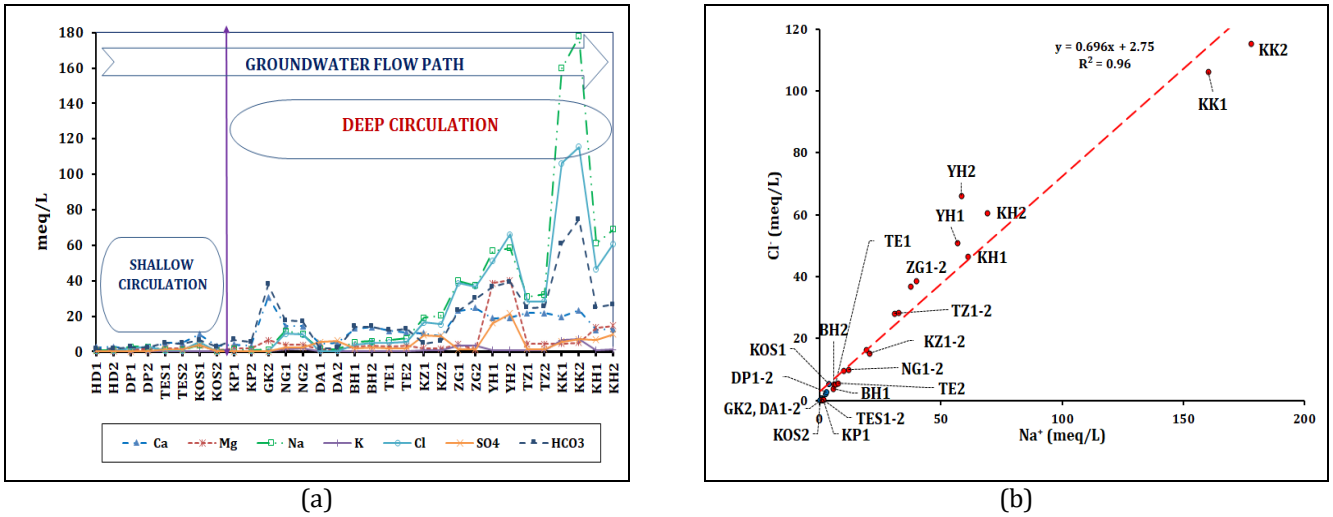

(a) (b)

Figure 3. (a): Ionic evolution along the groundwater flow path, (b): Na-Cl scatter diagram. Cold waters are shown in blue-filled circles, and geothermal waters are shown in red-filled circles. Other abbreviations are as in Table 1.

Therefore, KK appears to be the longest circulating water (Figure 3b). The dominant ions in the waters, such as Na+, may have entered due to the increased solubility of albite in volcanic rocks, as well as ion exchange between Na^{+} and Ca^{2+} or Mg^{2+} during interactions with tuff, claystone, sandstone, and/or syenite and granite [14],[8]. All geothermal waters, except DA, are mostly saturated with hematite, goethite, chalcedony, calcite, dolomite, aragonite minerals, and tend to precipitate them; they are not saturated with gypsum, halite, or anhydrite minerals, and tend to dissolve them [8].

Therefore, travertine precipitation has been observed in the source areas of the geothermal waters (TZ, ZG, NG, KZ, TE, KK, and KH), except for DA.

4.2 Evaluation of water isotope analyses

The results of water isotope analyses were used to evaluate the origin of both cold and geothermal waters in the study area (Table 2). This section presents an extensive assessment of the results of water isotope analyses.

4.2.1 $\delta^{18}O$ and $\delta^{2}H$ isotopes

The precipitation temperature, which is highly impacted by elevation, is primarily represented by the oxygen-18 ($\delta^{18}O$) and deuterium ($\delta^{2}H$) signatures of groundwater. Thus, stable isotope ratios are used as markers to estimate temperature and recharge altitude.

Table 2. Results of water isotope analyses and estimated ages.

Sample Symbol	$\delta^{18}O$ (‰ VSMOW)	$\delta^{2}H$ (‰VSMOW)	^{3}H (TU)	^{3}H error (TU)	Recharge altitude (m)	Recharge temperature (°C)	Discharge altitude (m)	Discharge temperature (°C)	^{14}C activity (pmc)	^{14}C activity error (pmc)	^{3}H age (year)	^{3}H age_error (year)	^{14}C age (ka)	^{14}C age error (ka)	Excess deuterium (d_{ex})	$\delta^{13}C$ (TDIC) (‰VPDB)	$\delta^{34}S$ (SO_4) (‰VCDT)
HD1	-11.45	-74.15	6.75	0.23	2564.68	3.07	1310	10.4	NA	NA	3.75	-0.033			17.5	NA	NA
HD2	-11.75	-73.28	8.1	0.33	2672.97	2.42	1310	10.4	9.98	0.15	0.5	0.081	15.27	0.123	20.7	1.6	NA
DP1	-11.95	-77.21	0.3	0.19	2748.22	1.97	1033	13	NA	NA	59.35	8.12			18.4	NA	NA
DP2	-11.75	-75.03	0.53	0.2	2674.80	2.41	1033	12.5	17.77	0.18	49.19	5.08	10.50	0.083	19.0	0.2	NA
TES1	-10.76	-73.66	4.52	0.21	2311.38	4.59	1022	12.5	NA	NA	10.91	0.179			12.4	NA	NA
TES2	-10.78	-72.88	5.05	0.31	2316.89	4.56	1022	13.3	NA	NA	8.93	0.432			13.3	NA	NA
KOS1	-9.8	-70.75	6.92	0.33	1958.98	6.71	1061	20	NA	NA	3.31	0.200			7.7	NA	NA
KOS2	-9.42	-67.95	8.63	0.36	1819.48	7.55	1058	12.8	NA	NA	-0.631	0.098			7.4	NA	NA
KP1	-11.45	-75.91	2	0.29	2564.68	3.07	1248	20.3	NA	NA	25.47	1.78			15.7	NA	NA
KP2	-11.04	-69.9	2.86	0.26	2414.17	3.98	1248	18.5	1.22	0.06	19.09	0.922	32.64	0.396	18.4	3.7	12.7
GK2	-11.22	-70.56	0.07	0.21	2480.25	3.58	1131	17.5	0.5	NA	85.34	24.12	40.01		19.2	9.5	20.9
NG1	-11.41	-76.94	1.49	0.17	2549.99	3.16	1375	61	NA	NA	30.73	-12.8			14.3	NA	NA
NG2	-11.16	-71.72	1.67	0.26	2456.38	3.72	1375	41	0.54	0.03	28.69	1.95	39.37	0.446	17.5	5.6	6.8
DA1	-11.58	-76.33	0.04	0.15	2612.40	2.79	1202	28.5	NA	NA	95.33	27.19			16.3	NA	NA
DA2	-11.60	-72.13	0.38	0.2	2619.74	2.74	1197	28.6	6.24	0.09	55.13	6.91	19.15	0.118	20.7	-1.4	10.4
BH1	-11.54	-80.9	-0.15	0.15	2597.71	2.88	1084	43.4	NA	NA	NA				11.4	NA	NA
BH2	-11.36	-75.04	0.49	0.2	2529.80	3.28	1084	42.2	2.31	0.06	50.59	5.48	27.36	0.211	15.8	4.3	15.2
TE1	-11.43	-78.53	0.55	0.21	2557.33	3.12	977	50.2	NA	NA	48.53	5.14			12.9	NA	NA
TE2	-11.31	-71.56	0.31	0.23	2513.28	3.38	977	54.3	2.38	0.08	58.76	9.27	27.12	0.273	18.9	1.2	14.9
KZ1	-10.98	-79.59	-0.38	0.21	2392.14	4.11	1056	86	NA	NA					8.3	NA	NA
KZ2	-10.95	-73.72	0.4	0.24	2379.30	4.19	1053	81.7	1.26	0.06	54.21	7.76	32.37	0.384	13.8	0.1	19.9
ZG1	-11.34	-80.92	0.8	0.18	2524.30	3.32	1270	45.4	NA	NA	41.83	2.99			9.8	NA	NA
ZG2	-11.31	-72.13	0.33	0.24	2513.28	3.38	1270	44.7	0.46	0.03	57.65	9.12	40.70	0.522	18.4	6.7	20.7
YH1	-11.81	-86.92	1.3	0.26	2696.83	2.28	1139	15	NA	NA	33.17	2.62			7.6	NA	NA
YH2	-11.75	-79.49	1.58	0.24	2674.80	2.41	1139	14.4	1.08	NA	29.68	1.89	33.65	0	14.5	6.1	5.5
TZ1	-9	-67.8	2.63	0.27	1665.31	8.47	1036	25.9	NA	NA	20.58	1.11			4.2	NA	NA
TZ2	-8.97	-59.83	2.64	0.28	1654.29	8.54	1036	25.4	2.54	0.08	20.51	1.16	26.58	0.256	11.9	6.3	16.9
KK1	-11.17	-85.3	0.99	0.23	2461.89	3.69	987	16.9	NA	NA	38.03	3.09			4.1	NA	NA
KK2	-10.86	-77.75	0.15	0.23	2348.09	4.37	1066	14.4	0.27		71.73	15.96	45.10		9.1	8.4	23
KH1	-10.1	-70.73	1.35	0.16	2069.10	6.05	1094	14.8	NA	NA	32.49	1.36			10.1	NA	NA
KH2	-10.13	-63.64	0.64	0.2	2078.28	5.99	1097	15.6	4.29	0.08	45.82	4.22	22.25	0.152	17.4	5.2	18.1

Abbreviations: TU: Tritium unit, pmc: percent modern carbon. TDIC: Total dissolved inorganic carbon, ka: kilo annum, NA: not available. Others are as in Table 1.

As elevation increases and/or recharge temperature decreases, precipitation becomes increasingly depleted in $\delta^{18}O$ and $\delta^{2}H$. Stable isotope signatures can display slight inter-annual fluctuations even for waters originating from the same recharge zone [10],[15].

$\delta^{18}O$ and $\delta^{2}H$ relations of the groundwaters and meteoric water lines are shown in Figure 4. Global Meteoric Water Line (GMWL) [16], as well as the local meteoric water lines for Ankara (Ank MWL), Adana (Ad MWL), and Antalya (Ant MWL) [17] are defined in cold waters, $\delta^{18}O$ values (‰) vary between −11.95 and −9.42, while $\delta^{2}H$ values range from −77.21 to −67.95. In geothermal waters, $\delta^{18}O$ values (‰) fall between −11.81 and −8.97, and $\delta^{2}H$ values range from −86.92 to −63.6 (Table 2).

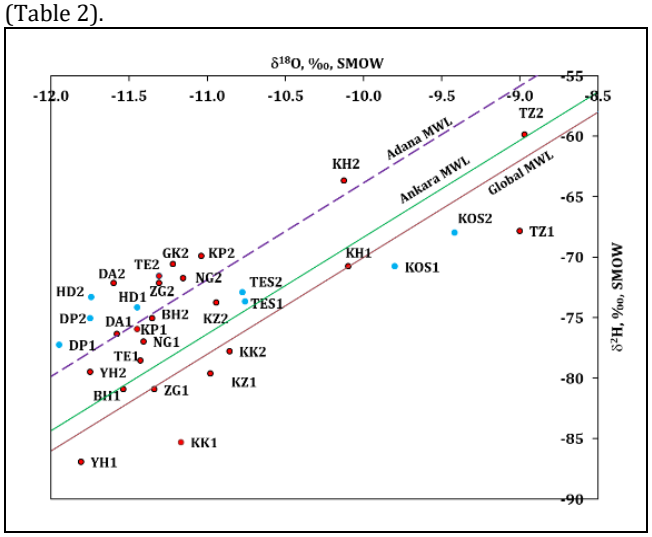

Figure 4. Scatter plot of $\delta^{18}O$ versus $\delta^{2}H$ for the water samples (Global Meteoric Water Line: 8* $\delta^{18}O$+10, Ankara MWL= 8* $\delta^{18}O$+11.68, Adana MWL= 8* $\delta^{18}O$+16.15, Antalya MWL= 8* $\delta^{18}O$+17.68 [17]. Cold waters are shown in blue-filled circles, and geothermal waters are shown in red-filled circles. Other abbreviations are as in Table 1.

YH1, KK1, KZ1, KK2, KOS1-2, and TZ1 plot below the GMWL and exhibit deuterium excess (d_{ex}) values lower than 10. The precipitation in the region where these waters originate may indicate that the area is humid. The ZG1 and KH1 plot directly on the GMWL, while BH1 and TZ2 lie along the Ank MWL. The YH2, TE1, KP1, NG1, BH2, KZ2, and TES1-2 plot between the Ad MWL and Ank MWL. The DA1 lies on the Ad MWL. The DP1-2, HD1-2, DA2, TE2, ZG2, GK2, and KP2 are located above Ant MWL, while HD1, NG2, and KH2 lie directly on the Ant MWL. The YH2, TE1, KP1, NG1, BH2, KZ2, and TES1-2 plot between the Ad and Ank MWLs. The DA1 lies on the Ad MWL. The DP1-2, HD1-2, DA2, TE2, ZG2, GK2, and KP2 are located above Ant MWL, while HD1, NG2, and KH2 lie directly on the Ant MWL. The precipitation in the region where these waters originate may indicate that the area is humid. d_{ex} values greater than 10 may indicate that the precipitation in the region where these waters originate is from an arid area. The fact that $\delta^{18}O$ values of cold and geothermal waters are more negative in the rainy season than in the dry season may indicate that these waters have undergone Rayleigh-type isotopic fractionation.

In this regard, elevated vertical deviations in $\delta^{2}H$ values for waters from DA, ZG, YH, KZ, and KH may reflect isotopic fractionation associated with dissolved hydrogen sulfide in these samples. According to the results of isotope analysis ($\delta^{18}O$, $\delta^{2}H$, ^{3}H), all waters are of meteoric origin.

All waters are associated with the GMWL, Ank MWL, Ad MWL, and Ant MWL. Datasets for many years on precipitation isotope composition and ground temperature from the meteorological stations in Ankara, Adana, and Antalya are reported in [17] (Table 3).

Table 3. Data in Adana, Ankara, and Antalya meteorological stations [17].

Station Name	Mean of amount weighted $\delta^{18}O$ (‰) value of annual precipitation	MAAT (°C)	Elevation of Station (m, asl)
Ankara	- 6.91	13.01	902
Adana	- 4.54	18.76	73
Antalya	- 4.73	17.45	49

$\delta^{18}O$ values in groundwater can indicate the average elevation and temperature at the time of recharge, assuming the original isotopic signature of the precipitation has remained unchanged since infiltration. An intense linear relation is observed between the elevation of the stations and the longstanding annual $\delta^{18}O$ values weighted by precipitation amount (Equation 1).

Furthermore, mean annual air temperature (MAAT) (°C) shows a strong dependence on station elevation (m). Recharge elevations and temperatures of the waters were calculated with the $\delta^{18}O$ values by using 1 and 2 equations (Table 3 and Figure 4).

$$\text{Elevation (m, above sea level)} = -367.09 \times \delta^{18}O - 1638.50 \quad (r^2 = 0.990) \tag{1}$$

$$\text{MAAT} = -0.006 \times \text{altitude} + 18.46 \quad (r^2 = 0.941) \tag{2}$$

Geothermal waters exhibit recharge temperatures of 2.28–8.54 °C, corresponding to recharge elevations of 1654–2696 m above sea level (asl). Cold waters generally show recharge temperatures of 1.97–7.55 °C, with recharge elevations ranging from 1819 to 2748 m (Figure 5).

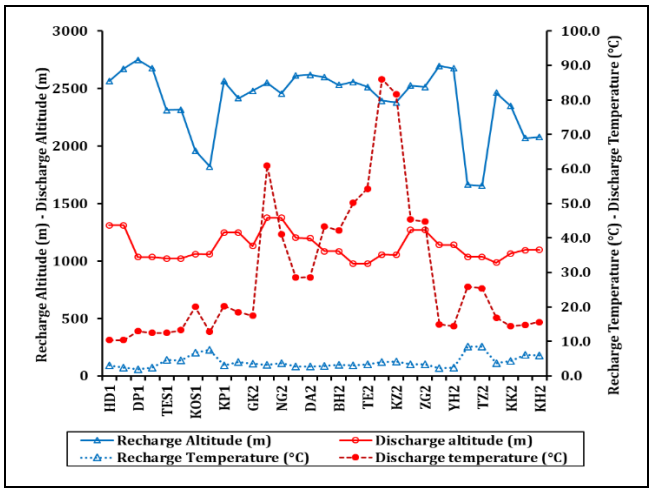

Figure 5. The changes in temperatures and elevations of recharge and discharge for water samples. Abbreviations are as in Table 1.

The cold and geothermal waters are generally recharged from higher elevations. The highest recharge altitude and recharge temperature in cold waters belong to the DP and HD; in thermal waters, to the YH; and the lowest recharge altitude and recharge temperature in cold waters belong to the KOS and the TZ (Table 3 and Figure 5).

4.2.2 Apparent age results for ^{3}H and ^{14}C isotopes

Radioactive isotopes such as tritium (^{3}H) and radiocarbon (^{14}C) are commonly applied for groundwater age estimation, respectively. Tritium is used to date relatively young waters, while radiocarbon is applied to much older waters. Tritium dating can resolve groundwater ages up to ~150 years [18], whereas radiocarbon dating is effective up to about 50,000 years [10, 15, 18, 19]. Apparent groundwater ages in this study were estimated using a piston-flow model, which assumes that successive recharge events remain unmixed and move sequentially through the aquifer like pistons in a cylinder. Although this assumption oversimplifies natural flow conditions—and thus apparent ages often underestimate true residence times—the model enables meaningful comparisons of relative groundwater ages within the same hydrogeologic system.

Apparent ages were calculated using the radioactive decay equation (Equation 3).

$$A_t = A_0 \exp^{-\lambda t} \quad (3)$$

Where:

A_0 represents the original activity of the isotope at the time it first entered the aquifer. A_t indicates isotope content in the water, λ denotes the radioactive decay constant (0.0564 year^{-1} of ^{3}H and 0.000121 year^{-1} of ^{14}C), and t refers to the circulation time of the water within the aquifer. In Equation 4, A_0 is not directly measurable, but the highest ^{3}H and ^{14}C values within the dataset were considered as A_0. For this purpose, the ^{3}H value of KOS2 (8.63 TU) and the ^{14}C value of the Şekerpınarı spring (63.33 pmc, as reported in [8]) were adopted as A_0 values in calculating the apparent ages based on ^{3}H and ^{14}C. Subsequently, Equation 4 was reformulated into the structure of Equation 3 to obtain apparent ages.

$$T = \ln\left(\frac{A_t}{A_0}\right)/(-\lambda) \quad (4)$$

Tritium concentrations in cold waters change from 0.3 to 8.63 TU, whereas geothermal waters exhibit much lower values, between −0.15 and 2.86 TU. In cold waters, radiocarbon activities range from 9.98 to 17.7 pmc, indicating that these waters are essentially unaffected by carbonate mineral dissolution. The geothermal waters display lower radiocarbon activities (0.27–6.24 pmc) compared to cold waters. This reduction, like that of tritium, records substantial isotope loss via radioactive decay along longer and deeper groundwater flow paths. Apparent tritium ages of cold waters range from 1.13 years (HD2) to 59.99 years (DP1), whereas geothermal waters yield ages of 19.72 years (KP2) to 95.97 years (DA1). Some geothermal samples with relatively high radiocarbon activities but low tritium contents (DA2 and KH2; Table 2) suggest mixing between young, shallow groundwater and older geothermal water (Figure 6).

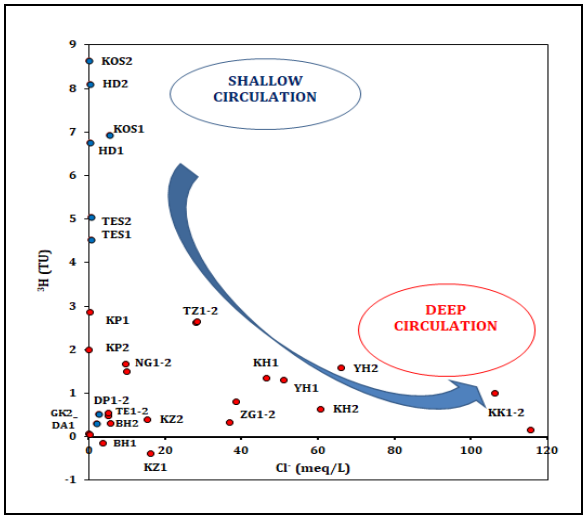

Figure 6. ^{3}H and Cl relationships of the water samples. The symbols are as in Figure 4, and the other abbreviations are as in Table 1.

Radiocarbon apparent ages for geothermal waters change between 19.15 ka (DA2) and 45.11 ka (KK2), indicating prolonged residence within the geothermal aquifer. The very low radiocarbon activities observed in certain geothermal samples (KK2, ZG2, NG2, GK2) further suggest recharge along the late Pleistocene to early Holocene.

The $\delta^{13}C$ composition (‰PDB) of dissolved inorganic carbon (DIC) is a valuable tracer for identifying CO_2 sources in groundwater. Key sources of DIC include atmospheric CO_2, root respiration, biogenic-thermogenic CH_4, fossil fuel emissions, mantle degassing, metamorphic processes, and the dissolution of carbonate minerals. The $\delta^{13}C$ value of atmospheric CO_2 is approximately −6.4. The type of photosynthesis in the vegetation changes the $\delta^{13}C$ value of root-derived CO_2. Photosynthetic pathway of the vegetation changes the root-originated. The $\delta^{13}C$ values for HD and DP are 0.2‰ and 1.6‰ PDB, respectively, while geothermal waters display a wider range from −1.4‰ (DA2) to 9.5‰ PDB (GK2). The main ^{13}C sources in HD, DP, and DA are interpreted as freshwater carbonates (Table 2 and Figure 7).

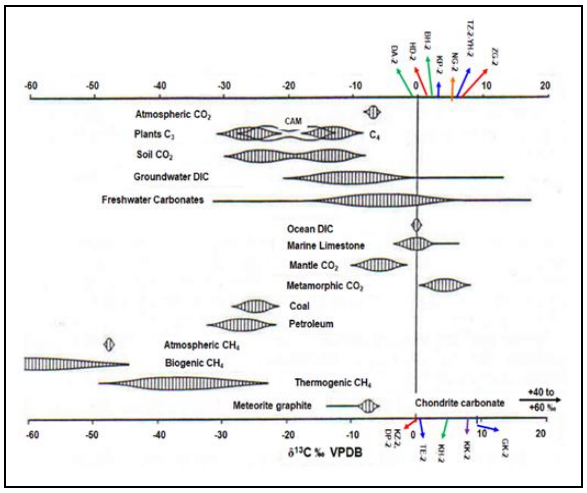

Figure 7. Sources of CO_2 to $\delta^{13}C$ contents of the waters for [10].

In general, the CO_2 within the analyzed waters is derived from freshwater or lacustrine carbonates of Late Miocene age, marine carbonates of Eocene age, and metamorphic rocks (Paleozoic Bozçaldağ marbles). The $\delta^{13}C$ compositions of geothermal waters suggest that the dissolved inorganic carbon (DIC) reflects a mix of crustal and mantle inputs. Considering the extensive Quaternary volcanism across central and western Anatolia [3], a geogenic origin of CO_2 is likely. These results indicate that the primary aquifer of the geothermal system is composed of marbles, while the secondary aquifer is made up of limestones. The exposure of marble and limestone in areas such as TZ, ZG, BH, TE, KZ, GK, and KK further supports this interpretation.

Sulfur is primarily found in the form of sulfate and sulfide minerals, dissolved sulfate and sulfide species, as well as hydrogen sulfide gas. The $\delta^{34}S$ isotope exhibits considerable fractionation through both biogenic and abiogenic processes in subsurface environments [15, 20]. $\delta^{34}S$ values vary between 6.1‰ in YH and 8.4‰ in KK2 (Table 2). Sulfate concentrations range from 6.88 meq/L in KK2 to 21.62 meq/L in YH2. The elevated SO_4^{2-} levels observed in YH2, KH2, KZ2, KK2, and DA2 are likely related to extended exposure to the atmosphere during surface discharge [21]. The SO_4^{2-} present in KK2, ZG2, KZ2, TZ2, and KH2 originates mainly from marine evaporitic minerals (gypsum), whereas in other waters it is derived from volcanic, coal, and/or carbonate rocks of Cenozoic to Devonian–Permian age. In this context, [22] reported that the $\delta^{34}S$ compositions of sulfate minerals in Mekedere and Kükürtdere (Güzelyurt - Aksaray) indicate that SO_4^{2-} primarily originated in steam-heated (H_2S oxidation) and magmatic-hydrothermal environments with limited sulfur isotope exchange between SO_4^{2-} and H_2S. (Table 2 and Figure 8).

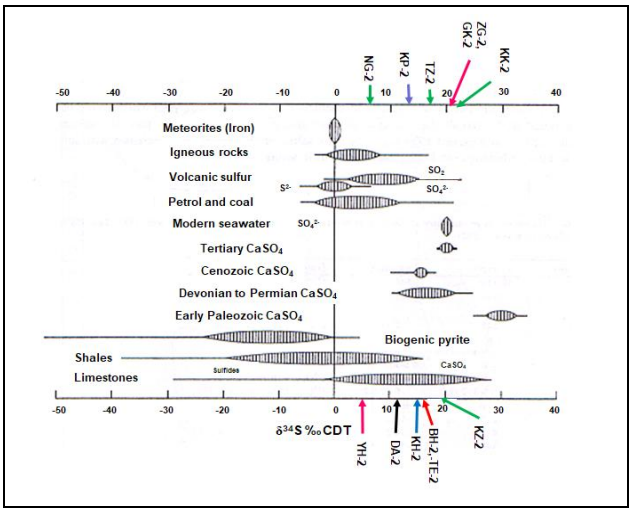

Figure 8. Sources of SO_4^{2-} to $\delta^{34}S$ contents of the waters for [10].

5 Conclusions

In this study, some important carbonated, sulfated, and saline geothermal waters in Central Anatolia were evaluated in terms of their origins with the help of hydrogeochemistry and isotope properties. The geothermal waters of GK, KP, DA, TE, KZ, BH, KK, TZ, ZG, NG, YH, and KH, where temperatures range from 17.5 to 86 °C, and to evaluate their origins, taking into account the cold waters of HD, DP, TES, and KOS, where temperatures range from 10.4 to 13.09 °C. in Central Anatolia. The aquifers of these fault-controlled waters are of Paleozoic marbles and Eocene limestones; cover rocks are impermeable units. The heat production system of these waters may be due to young volcanism and granitic/syenitic intrusions as well as radiogenic sources. The types of these carbonated, sulfated, and saline waters are Ca-HCO_3 in KP, GK, BH, and TE; Na-SO_4 in KZ; Ca-SO_4 in DA; Na-Cl in TZ, ZG, NG, KH, and YH, respectively. All geothermal waters, except DA, are mostly saturated with hematite, goethite, chalcedony, calcite, dolomite, and aragonite minerals, and tend to precipitate them; they are not saturated with gypsum, halite, or anhydrite minerals, and tend to dissolve them.

All waters, which are of meteoric origin in terms of isotopic ($\delta^{18}O$ and $\delta^{2}H$). Geothermal waters generally have deep circulation and slow flow. The main reason for the deviation observed from the meteoric water line in some waters is evaporation. Geothermal waters show recharge temperatures of 2.28–8.54 °C, corresponding to elevations of 1654–2696 m asl. Cold waters, by comparison, have recharge temperatures of 1.97–7.55 °C and recharge elevations between 1819 and 2748 m (asl). The cold and geothermal waters are generally recharged from higher elevations. The highest recharge altitude and recharge temperature in cold waters belong to the DP and HD.

Radiocarbon contents in geothermal waters (0.27–6.24 pmc) are lower than those in cold waters. Apparent tritium ages for geothermal waters range from 19.72 years (KP2) to 95.97 years (DA1). The presence of high radiocarbon activities alongside low tritium levels in some geothermal samples (DA2 and KH2) suggests mixing between young cold groundwater and older geothermal water.

Variations in Na/Cl ratios and dissolved oxygen (DO) levels from younger to older waters reflect the duration of water–rock interaction, increasing circulation depth along the groundwater flow path, and the water's mixing feature. The causes of salinization in the Na-Cl-type waters may be the dissolution of halite minerals and the mixing of older waters trapped at depth during the closure of the Tuzgölü and salt domes in the TZ and ZG, the Central Kızılırmak basin in the YH and KK, and the Ulukışla basin in the KH.

^{14}C values of the waters are not real ages of the waters, but they are measures of the contribution of modern biogenic carbon in total dissolved carbonate or bicarbonate. ^{14}C apparent values of the waters are increasing from young waters to old waters, whereas per cent modern (pmc) carbon values are decreasing in the same order. The sources of CO_2 in the waters may suggest freshwater carbonate, marine carbonate, and metamorphic, according to the results of $\delta^{13}C$. The origins of $\delta^{34}S$ in the waters may be atmospheric, evaporitic, volcanic, and/or carbonate rocks.

According to $\delta^{13}C$ (‰PDB) values, the sources of CO_2 gas in waters may be geogenic (marble, marine and lacustrine limestone) and/or mantle. According to $\delta^{34}S$‰VCDT values, the source of sulfate in waters may be evaporitic rocks in KK, ZG, KZ, TZ, KH; volcanic (NG, KP, DA) and/or carbonate rocks in BH, TE, and YH. The ^{14}C ages of the waters are lowest in DA (19.15 ka) and highest in KK (45.11 ka). The calculated ages are apparent because the ^{14}C values of the waters in question are often a measure of the contribution of modern biogenic carbon to the total dissolved carbonate or bicarbonate. In this context, the waters examined may be old waters that entered the system during the late Pleistocene and early Holocene periods.

6 Author contribution statements

For this study, Mustafa Afşin, Mustafa Murat Kavurmacı, Ali Gürel, Ümmühan Gökçen Duru, and Özcan Oruç contributed to the field, laboratory work, literature review, conduct of the experiments, and the evaluation of the obtained results.

7 Ethics committee approval and conflict of interest

"There is no need for ethics committee approval for the prepared article". "There is no conflict of interest with any person/institution in the prepared article".

8 References

[1] Mutlu H, Gulec N. "Hydrogeochemical outline of thermal waters and geothermometry applications in Anatolia (Turkey)". *Journal of Volcanology and Geothermal Research*, 85, 495–515, 1998.

[2] Afşin M, Allen DA, Kriste D, Durukan ÜG, Gürel A, Oruç O. "Mixing processes in hydrothermal spring systems and ımplications for interpreting geochemical data: a case study in the cappadocia region of Turkey". *Hydrogeology Journal*, 22(1), 7-23, 2014.

[3] Afşin M, Bayarı CB, Dağ T, Davraz A, Aksever F, Karakas Z, Hınıs MA. "Conceptual hydrogeological model of the Hüdai Geothermal Field (Afyonkarahisar, Turkey) based on hydrochemical and environmental isotopic data". *Hydrogeology Journal*, 33(3), 755–779, 2025.

[4] Çağlar KÖ. *Türkiye Maden Suları ve Kaplıcaları.* MTA Enstitüsü Yayınları, Ankara, Türkiye, Seri B, No: 11, 1950.

[5] Afşin M, Baş H. "Hydrochemical evaluation of the Koçpınar springs (Aksaray), central Anatolian, Turkey". *Geological Bulletin of Turkey*, 39(1), 69–80, 1996.

[6] Gazioğlu M. "Oral communication". DSİ Genel Müdürlüğü 4. Bölge Müdürlüğü, Konya, Türkiye, 20.10.2025.

[7] Afşin M, Gürdal H. "Ihlara vadisi ve çevresindeki (Ziga, Yaprakhisar, Belisırma, Ihlara, Ilısu) Jeotermal Suların Tıbbi-Biyoiklimsel ve Hidrojeokimyasal İncelemesi, Aksaray, Türkiye". Proje No: ASÜ BAP FEB 2020-2021, 2022.

[8] Afşin M, Erdoğan N, Gürdal H, Gürel A, Onak A, Oruç Ö, Kavurmacı M, Durukan G. "Orta Anadolu'daki sıcak ve mineralli suların ve travertenlerin hidrojeokimyasal ve izotopik incelenmesi ve suların tıbbi ve biyoiklimsel değerlendirilmesi, Aksaray, Türkiye". Ankara, Türkiye, TÜBİTAK Proje No: ÇAYDAG 104Y197, 2007.

[9] Lefebvre C, Barnhoorn A, Hinsbergen VD, Kaymakci N, Vissers RLM. "Late Cretaceous extensional denudation along a marble detachment fault zone in the Kırsehir massif near Kaman, central Turkey". *Journal of Structural Geology*, 33, 1220-1236, 2011.

[10] Clark ID, Fritz P. *Environmental Isotopes in Hydrogeology*. 1st ed. Boca Raton, FL, USA, CRC Press, 1997.

[11] APHA (American Public Health Association), AWWA (American Water Works Association), and WPCF (Water Pollution Control Federation). "Standard Methods For The Determination of Water and Waste Water". APHA, Washington, DC, USA, 15th ed. 1995.

[12] Freeze RA, Cherry JA. Groundwater. 1st Ed. Prentice Hall, Englewood Cliffs, NJ, USA, 1979.

[13] Afşin M. "CO_2'ce zengin Çorak, Karakaya ve Gümüşkent (Nevşehir) mineralli sularının hidrojeokimyası". *Yerbilimleri, HÜ Yerbilimleri Uygulama ve Araştırma Merkezi Bülteni*, 26, 1-14, 2002.

[14] Afşin M, Kuşcu İ, Elhatip H, Dirik K. "Hydrogeochemical properties of CO_2-rich thermal-mineral waters in Kayseri (Central Anatolia), Turkey". *Environmental Geology*, 50(1), 24-36, 2006.

[15] Clark ID. *Groundwater Geochemistry and Isotopes*. 1st ed. Boca Raton, FL, CRC, 2015.

[16] Craig H. Isotopic variations in meteoric waters. *Science*, 133(3465), 1702–1703, 1961.

[17] Dilaver AT, Aydın B, Özyurt NN, Bayarı CS. *Türkiye yağışlarının izotop içerikleri (2012-2016).* Devlet Su İşleri Genel Müdürlüğü Teknik Araştırma ve Kalite Kontrol Dairesi Başkanlığı ve Meteoroloji Genel Müdürlüğü Araştırma Dairesi Başkanlığı. Ankara, Türkiye, 2018.

[18] Özyurt NN. "Residence time distribution in the Kırkgöz karst springs (Antalya–Turkey) as a tool for contamination vulnerability assessment". *Environmental Geology*, 53, 1571–1583, 2008.

[19] Cartwright I, Currell MJ, Cendón DL, Meredith KT. "A review of the use of radiocarbon to estimate groundwater residence times in semi-arid and arid areas". *Journal of Hydrology*, 580, 124–247, 2020.

[20] Wei Z, Huang S, Xu J, Yuan C, Zhang M, Wang C. "Geochemical evolution of geothermal waters in the Pearl River Delta region, South China: insights from water chemistry and isotope geochemistry". *Journal of Hydrology*, 51, 101670, 2024.

[21] Yıldırım N, Güner İN. "Büyük Menderes Grabeni'nin doğusunda yeralan jeotermal sahalarda bulunan suların izotopik ve hidrojeokimyasal özellikleri". *DSİ TAKK Dairesi Başkanlığı, 2. Hidrolojide İzotop Tekniklerinin Kullanılması Sempozyumu*, Adana, Türkiye, 21-25 Ekim 2002.

[22] Çelik Karakaya M, Karakaya N, Temel A, Yavuz F. "Mineralogical and geochemical properties and genesis of kaolin and alunite deposits SE of Aksaray (Central Turkey)". *Applied Geochemistry*, 124, 1-13. 2021.